Mechanical Systems and Signal Processing 85 (2017) 1020–1034

Contents lists available at ScienceDirect

Mechanical Systems and Signal Processing

journal homepage: www.elsevier.com/locate/ymssp

Control of deviations and prediction of surface roughness from micro machining of THz waveguides using acoustic emission signals

James M. Griffin[a,*], Fernanda Diaz[b], Edgar Geerling[b], Matias Clasing[b], Vicente Ponce[b], Chris Taylor[e], Sam Turner[e], Ernest A. Michael[c], F. Patricio Mena[c], Leonardo Bronfman[d]

[a] Mechanical Automotive and Manufacturing, Faculty of Engineering And Computing, Coventry University, Priory Street, Coventry CV1 5FB, UK
[b] Mechanical Engineering Department, FCFM, University of Chile, Beaucheff 851, Santiago, Chile
[c] Electrical Engineering Department, FCFM, University of Chile, Av. Tupper 2007, Santiago, Chile
[d] Astronomy Department, FCFM, University of Chile, Camino Observatorio 1515, Santiago, Chile
[e] AMRC with Boeing, The University of Sheffield, Wallis Way, Catcliffe, Rotherham S60 5TZ, UK

ARTICLE INFO

Keywords:
Acoustic emission
Precision manufacturing
Surface finish
Precision control
Submillimetre waveguide manufacturing
CART
Neural networks and simulations

ABSTRACT

By using acoustic emission (AE) it is possible to control deviations and surface quality during micro milling operations. The method of micro milling is used to manufacture a submillimetre waveguide where micro machining is employed to achieve the required superior finish and geometrical tolerances. Submillimetre waveguide technology is used in deep space signal retrieval where highest detection efficiencies are needed and therefore every possible signal loss in the receiver has to be avoided and stringent tolerances achieved. With a sub-standard surface finish the signals travelling along the waveguides dissipate away faster than with perfect surfaces where the residual roughness becomes comparable with the electromagnetic skin depth. Therefore, the higher the radio frequency the more critical this becomes. The method of time-frequency analysis (STFT) is used to transfer raw AE into more meaningful salient signal features (SF). This information was then correlated against the measured geometrical deviations and, the onset of catastrophic tool wear. Such deviations can be offset from different AE signals (different deviations from subsequent tests) and feedback for a final spring cut ensuring the geometrical accuracies are met. Geometrical differences can impact on the required transfer of AE signals (change in cut off frequencies and diminished SNR at the interface) and therefore errors have to be minimised to within 1 μm. Rules based on both Classification and Regression Trees (CART) and Neural Networks (NN) were used to implement a simulation displaying how such a control regime could be used as a real time controller, be it corrective measures (via spring cuts) over several initial machining passes or, with a micron cut introducing a level plain measure for allowing setup corrective measures (similar to a spirit level).

* Corresponding author.
E-mail addresses: James.griffin2@coventry.ac.uk (J.M. Griffin), emichael@ing.uchile.cl (E.A. Michael).

http://dx.doi.org/10.1016/j.ymssp.2016.09.016
Received 25 November 2015; Received in revised form 14 June 2016; Accepted 10 September 2016

1. Introduction

Micro machining is a necessary process for manufacturing astronomical instrumentation as very small geometries are required with a defect free and smooth surface finish. Micro machining is a difficult process to carry out as the tool structure is susceptible to unwanted vibration due to less stiffness (small diameter and large length), which can result in poor surface quality and out of tolerance dimensions. By using AE, the signal is directly related to the micro-mechanical activities of the cutting process. Due to AE being concerned with high frequencies (ultrasound, our model is sensitive in the range of 0.1–1 MHz) the lower-frequency machine vibrations and environmental noise can be filtered out at no great cost. AE has already seen uses in tool condition monitoring, detection of work piece surface defects and chip management [1]. As a continuous signal source, AE can be used to monitor the following [1]:

- Plastic deformation in the workpiece.
- Plastic deformation in the chip.
- Tool-chip sliding friction (frictional contact between the tool rake face and the chip resulting in crater wear).
- Tool-workpiece sliding friction (frictional contact between the tool flank face and the workpiece resulting in flank wear).

As a transient AE signal source the following can be monitored for:

- Collisions between the chip and tool.
- Entanglement of chips.
- Tool fracture.
- Chip breakage.

Micro machining processes for astronomical instrumentation are particularly sensitive to the surface roughness and, the precision of achieved machining geometrical accuracies.

The current tolerance of the tailored micro machine setup is optically measured as 4 μm (See Figs. 1 and 2). The idea behind using a precision sensing capability is to achieve a precision of 1 μm, as the specified precision of the used micro machine was 1 μm over small areas. However, the main problem with the current setup is that the initial zero machine table datum is provided by visual inspection via an optical microscope (similar to work referenced in [2]). Where the machine probe is used to give the X, Y Z 0 position and confirm the setup accuracy of the machined part. Gauge markers on the fixture are then used for repeat setup purposes. If an inaccuracy is found with the setup then the probe position should pick this up and by using the gauge markers and optical microscope to correct any found errors. Even with such setup methodologies there can still be an associated error which can increase if not corrected. The proposed idea: deduce information from Acoustic Emission (AE) measurements that could lead to identify errors in-situ and give corrective machine commands to counter balance against setup and other machining inaccuracies (Fig. 3).

This idea of using closed feedback control is particularly important as most machining platforms have associated in/decreasing setup errors due to environmental changes, technology use/access and tool condition to name a few [2]. The work discussed here was carried out at the University of Chile´s Astronomy Department´s Millimeter-Wave Laboratory at the top of a hill: Cerro Calán in Santiago (this environment is very dry and hot in the January months with occasional seismic activity that can add to increasing errors). Another problem obtained in CNC precision is that of achieved control versus desired control where actuator backlash, wearing of gears can all add to the problems of deviations. Other problems were obtained in micro milling where push off and vibrations occur which are based on the large tool length to small diameter ratios: such problems only add to the problems of increased geometrical inaccuracies. Finally, another problem to be considered is in terms of temperature gradients that can impact on material machining accuracy. In the carried out tests the micro machine working area was kept at a constant temperature through closed loop control/thermostat.

Another important reason for using AE sensor technology is to make sure that the process is free from mechanical disturbances like resonance vibrations. This is very important in micro-machining applications, where spindle speeds have to be very high due to

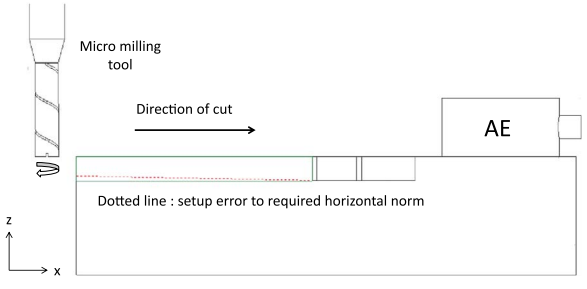

Fig. 1. A schematic of the machine setup and associated errors.

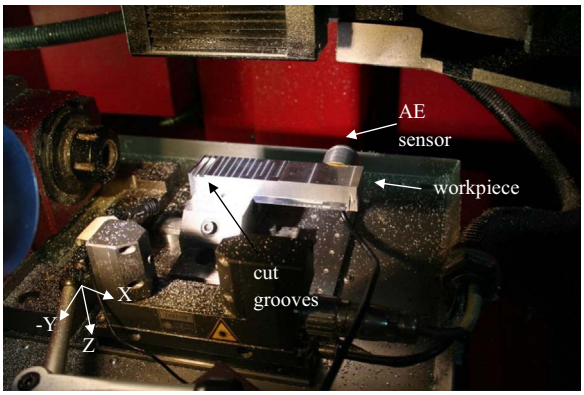

Fig. 2. An image of machine setup to pick up off level setup errors using AE sensors.

the small tool diameter for example [3]. Due to high spindle speeds, micro-milling tools wear at a high rate, with cutting forces rising (this is also correlated to an increase in AE see Fig. 4 for an example of this) as the tool wear increases [4] which is critical for identifying the onset of tool malfunction/tool dimensional change.

When carrying out precision machining there is a need to control processes through various feedback signals that are both accurate and sensitive to change. One of such sensor technologies that can be applied to accurate precision control is AE. With such sensitive sensing capabilities and a lack of standardisation there is a need to calibrate AE to standardised energy quantities or, to calibrate daily against a reference phenomenon with a relatively constant energy pattern, such as the breaking of a graphite fibre pencil [5]. This was carried out during previous work [6] where AE sensitive to minute material dislocations and/or interactions were correlated to force measurements (AE sensor can also be used to indentify relative loads).

There is other related work using AE for monitoring tool wear with the addition of force signals where both are introduced to supervised back propagation and unsupervised Adaptive Resonance Theory Neural Networks (NNs) to distinguish salient AE Fast Fourier Transform (FFT) features experienced during insert wear when turning [7]. Jemielniak investigates this further by correlating AE measurements with insert wear promoting more generalised learning capabilities with adaptive biases between both training and test data, ensuring the NN does not get stuck in local minima [1]. Other work investigates wavelet transforms (WT) with a fuzzy-NN used to determine the wear states from correlated AE during drilling of 40Cr steel [8]. Venkatesh et al. [9] predicted insert wear through NN models using the input of time, velocity, feed and cutting force. Such work is useful for the research discussed in this paper due to the parallels between micro-milling and insert, single point cutting technology where multiple point cutting considers several inserts interacting. Sharma et al. [10] looks at more recent research where the measurement of cutting forces are used to provide prediction of the surface roughness for hard turning. When reviewing other literature [11] there is a direct relationship between force and AE which again is of particular relevance to the research presented here. Another recent investigation [11] looks at wear mechanisms and prediction of Material Removal Rate experienced during micro milling to quantify how AE can be used to distinguish such microscopic phenomena.

The research discussed in this paper utilises such ideas in identifying microscopic features through AE signals generated when shallow cuts are made whilst machining a submillimetre waveguide. Moreover, the precision of AE technologies applied to wear can

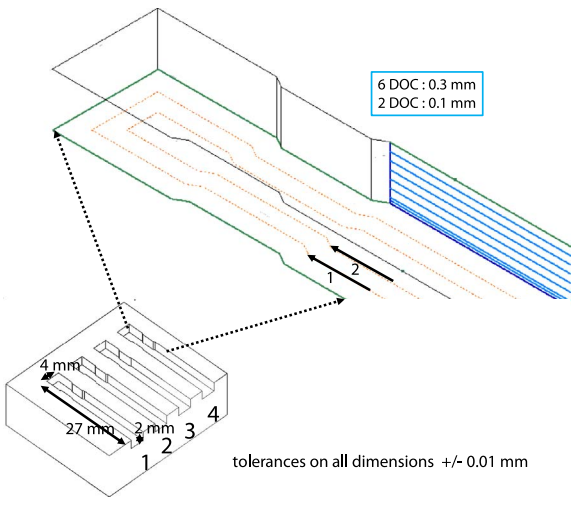

Fig. 3. A schematic displaying micro milling tool paths.

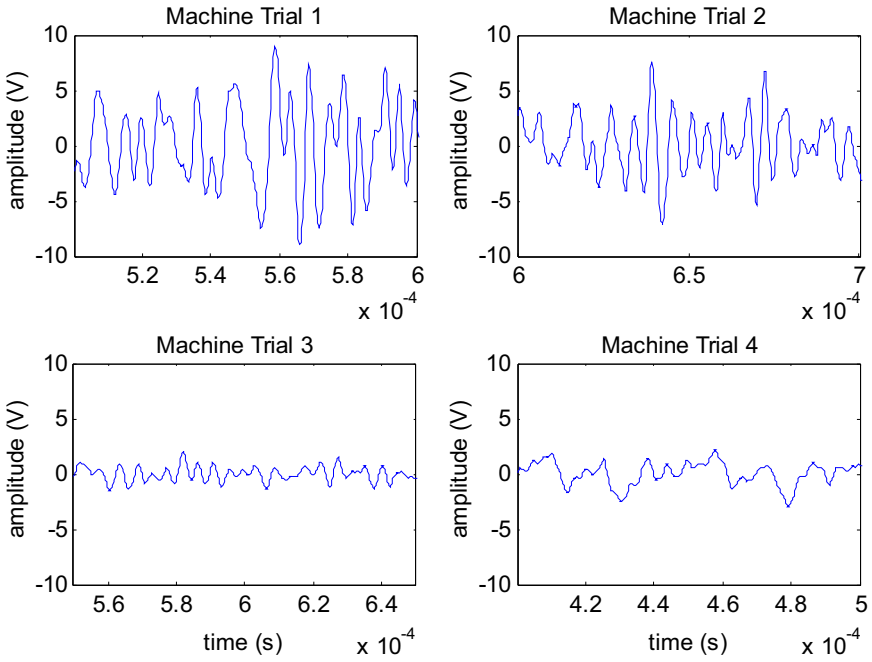

Fig. 4. Selected time series AE signals for 4 Tests. Tests 1 and 2 are performed with a worn tool, Tests 3 and 4 use new tools.

also be translated for measuring the distance between the tool tip and workpiece which is very important when considering micro machining operations (this could act as another measurement probe technology). This has been considered before in previous work [12] and can be seen here with further application where the sensor provided similar results to an inductive or capacitive probe. If the AE is post processed in a computationally affordable fashion, such salient information can be used to control the distance discrepancies in both real-time, and, to accurate levels [12]. Thereby giving a reactive control authority against the many sources of deviations already discussed.

Another important point to note here is that the use of a force sensor, requires its own calibration routine with a known force applied, and requires invasive fixture to the workpiece and machine centre. With AE sensors however, these can be stuck on by glue or other bonding methods and applied to the most difficult places to access.

The main investigation objectives of this paper are:

- Characterise the different levels of each phenomenon in terms of AE correlated to deviation (depth of cut (DOC)=0.3 mm for 6 passes and two finishing DOC=0.1 mm spring cuts where the last passes are the corrective DOCs).
- Characterise the deviation phenomena using both the time and frequency domain analysis of the AE gained during the vertical-axis micro milling tests.
- Characterise significant tool wear of micro milling after and before the onset of tool malfunction.
- Characterise the phenomena summaries into salient data groups for application to classifier.
- Classify different levels of the characterised phenomena for the prediction of surface quality.
- Produce a real-time simulation displaying changing energy patterns as deviation errors increase/decrease.

2. Precision methods for submillimetre waveguide fabrication

2.1. Submillimetre waveguide fabrication using micro-milling

In the facility of Cerro Calán at the University of Chile, submillimetre wave guides and other instrumentation for radio astronomical projects [13,14] are manufactured using a 5 axis KERN micro machine centre (see Section 5 for more information on the machine setup). Where the first results of the Sideband Separating Mixer for ALMA Band 9 Upgrade was carried out by Khudchenko et al. [14]. This machine is considered one of the most precision orientated micro machine centres available. However, with location and operating conditions as mentioned in the introduction, precision can be seriously compromised. In addition, to obtain a defect free surface a uniform quality surface is also required. Such requirements are for low-loss signal transmission permitting the investigations of high frequencies in the THz range (e.g. ALMA Band 9 [14]). If defects or non-uniformities exist on the surface they will constitute an additional resistance for the electrons if their size is comparable to or, larger than the penetration depth into the metal (“skin” depth) of the oscillating E-field at the sub-millimeter or THz frequency. Thus, the loss per unit length of the signal travelling along the waveguide will be increased.

Khan and Fartaj [15], Gunnasegaran [16] and Khadem [17] also affirm that the surface roughness is considered to be one of the most important factors for geometrical deviations as signals associated to deviations often dissipate, for example; when the channel dimension reduces, the importance of roughness increases.

2.2. Micro-milling measurements: surface quality and deviations

Narayanan et al. [18] used an electrical edge–finder probe [19] to determine the tool offsets for the edge of the workpiece. Moreover, Narayanan et al. talks about two issues of manufacture that impact on the waveguide functionality, namely, with milling tool cutters they require many tool changes which give rise to errors (this is certainly true for very small tool diameters) and employed temperature closed-loop control within the machine operating environment (within machine enclosure) ensures less material deviations occur due to changes being stable throughout machining. In addition, Narayanan et al. [20] discusses what impact the change in length and width of the alignment will have on the signal which is considered significant for just 2–5 μm misalignments. Narayanan et al. [20] also uses a microscope to see if the alignments of setup are accurate.

A study into the influence of the width of cut on micro milling aluminium alloys was made by [21] which are particularly important to the work discussed here. Mougo et al. investigated the importance of specific parameters in achieving the required surface finish for micro channels, with findings as follows; “size effect” in micro machining observed by Aramcharoen and Mativenga [22] which is characterised in machining as a non-linear increase in specific cutting energy (or specific cutting force) with decrease in undeformed chip thickness. Bao and Tansel [23] and Vollertsen et al. [24] presented a review on size effect and their use: the typology of size effect, a description of size effect on strength and, tribology and size effect on formability and machinability. Afazov et al. [25] studied the micro milling conditions on the cutting forces and process stability through the effects of tool wear, rake angle, run-out, workpiece material, and chip thickness. Malekian et al. [3] and Vogler et al. [26], discuss microstructure also has significant effect at the microscale cutting level. Lastly, Simoneau et al. [27] and Araujo et al. [28] studied the micro milling cutting forces on the machining of an aluminium alloy where experimental results were compared to the mechanistic model.

Bao and Tansel [23] discussed that the feed per tooth to tool radius ratio has to be higher than in conventional milling to keep productivity at a reasonable level. With low feed rates, when chip thickness is lower than the required minimum chip thickness there is no effective cut. Instead, the workpiece tends to be pushed and “crushed” by the tool where only rubbing or ploughing occurs. Griffin & Chen, [29] show rubbing and ploughing mechanisms can be detected by AE. Therefore, with the conditions presented in this work, it is recommended that the machining of the wave guide channel is carried out with a tool with a lower diameter as opposed to a variable width of cut for finishing. The AE sensor can also be used to see if the extracted signals are significant of cutting and producing chip or, just mealy rubbing and ploughing the material. When such recommendations are followed, care has to be placed in the increased possibility of chatter vibrations which can impact on both geometrical tolerances as well as surface finish (not to mention catastrophic tool failure).

2.3. Wear and deviation measurements using AE

The cross-correlations between the AE and wear phenomena are now compared to other AE signals and output phenomena. The AE is much larger in terms of bandwidth, signifying that the AE signal contains more information and can be considered independent from the other signals [3]. This is attributed to the fact that the AE signal can capture high-frequency vibrations which cannot be captured by other sensors [30].

The work by [31] looks at direct control where the power signal is used to identify when a change of tool should take place. Power signals can give different facets of information, where a drop in peak energy at a particular time interval can signify tool breakage and at the same time give information as to the location of the tool malfunction. On the converse, power data can lack resolution. The sensed power signal is somewhat similar to that of AE as they are both measuring energies albeit non-invasively where both could be used as non-evasive sensor fusion setup.

Jamielniak and Arrazola [32] used AE and cutting force signals for Tool Condition Monitoring (TCM). It was noticed that the AE signal undergoes prominent changes, being much stronger at the beginning and weaker towards the middle of a cut, often rising again at the end. These changes can be caused by different AE signal paths or, when the feed path changes direction away from the sensor. Similar findings were made during this work (only signals considered were obtained when the cutting path was towards the AE sensor). The duration of the tool–workpiece contact is so short however with an AE root mean squared signal (AE_{RMS}) the engagement contact between the tool and the workpiece was established. While the uncut chip thickness is so small, the cutting force signals almost do not react when extracted, the AE_{RMS} signal rises eminently up to 55 mV in 0.2 ms. This shows the AE_{RMS} signal to be a versatile means in detecting the contact between the tool and part, and in addition conveying the tool integrity.

It should be noted that since the diameter of miniature tools are very small, excessive forces and vibrations significantly affect the overall quality of the part and sensors such as accelerometers, force and AE can be used to monitor such phenomena [3]. With micro machining it is no longer valid to assume that with a sharp new tool the surface related to the applied DOC will be completely removed. Instead, with a small tool edge radius, and very low feed rates both ploughing and elastic recovery are significant. For instance, the edge radius is comparable to the chip thickness which is often associated to large negative rake angles. The elastic recovery of the material in micro-scale affects the tool wear by promoting fluctuations in forces (significant also to chipping from intermittent tool impacts which ultimately result in malfunction) and an increase in the tool contact area between the tool and workpiece: causing more friction and rubbing inherently, increasing flank wear. Also a point should be noted that the feed rate can be too low promoting unwanted resonant vibrations, where increased feed rates should ensure this is eliminated (low speeds are

more significant to build up edge/smearing and frequencies near the machine natural frequency). From carrying out real-time adaptive monitoring of the cutting process it is possible to predict the onset of tool malfunction before the tool gets to a critical state.

Marinescu and Axinte [33] present results from milling with an AE sensor which efficiently measures both tool malfunctions and workpiece surface anomalies. This work is made in comparison with more traditional sensor extraction techniques such as force and accelerations for TCM, which are considered more limited in terms of capability. In their work two major findings were made; firstly, when milling on circular tool paths orthogonal cutting forces (F_x and F_y) change sign during the complete tool pass which makes it very difficult to correlate increasing tool wear with specific forces and instead it was considered that a combination of the resultant force F_{xy} was more sensitive to change. The other finding: the force F_{xy} lacked the resolution to be able to observe the point when the cutting edge started and ended cutting. However when using AE sensors with STFT transformations it is possible to indentify the start and end of individual milling insert cutters. This work confirms the suitability of using an AE sensor to enable simultaneous monitoring of deviation inaccuracies and tool wear.

3. Intelligent precision control for machining 1 micrometre accuracies

3.1. CART rule based classification technique

The treeviewer classifier uses the CART algorithm to carry out classification. CART is particularly useful in segregating n-dimensional data sets and producing transparent, easily readable sets of classification rules. For this reason it is used here. CART however is a method of classification similar to fuzzy clustering, with the added facet of producing more transparent rules. By using pre-processing techniques in real-time, other classifiers are considered unsuitable based on the increase in computational complexity which impacts on processing in real-time.

CART builds classification and regression trees for predicting continuous dependent variables (regression) and categorical predictor variables (classification) [34]. It achieves its functionality by recursively splitting the feature space into sets of non-overlapping regions, and finally by predicting the most likely value of the dependent variable within each region. By generating a binary tree through recursive partitioning it splits the data into sub nodes based on the minimisation of a heterogeneity criterion computed at the resulting sub-nodes. With the CART algorithm the tree is forwardly propagated (using forward stepwise regression) for the best purity of node split. The best node split becomes the chosen value of partition (see Eq. (1)).

A good splitting criterion is as follows:

PRE =Ø(s, t).

Misclassification error:

$$Q_m = \frac{1}{N} \sum_{x_i \varepsilon R^m} (yi \neq k(m)) = 1 - \hat{P}_{mk(m)} \tag{1}$$

where y_i is the output of the individual under test and k(m) is the class category under test.

where PRE is the minimum production reduction in error and s is the split at any t node. The best purity measure looks at the best unique class classification where less impure looks at more multiclass representation. For the CART algorithm the percentage accuracy of classifications is used as a best purity measure.

This method of classification is chosen because the tree fitting methods are actually closely related to cluster analysis [35]. This is where each node can be thought of as a cluster of objects, or cases, that are split by further branches in the tree (providing if, then, and else rules). An easy to understand CART example can be found in Coppersmith et al. [36] where petal length and width are rule discriminators for a flower species dataset.

3.2. Precision controller

Rules can be a simple yet effective way to represent the classification of a given dataset. It should also be noted that classifier system rules give a more transparent output in terms of how the different data sets are segregated, providing further confidence to the obtained rules. Obtained rules from Fig. 9 are easily transferred into “if,” “elseif,” and “greater or less than” rules and can be coded into embedded systems for precision control. This type of classifier technique is new to condition monitoring, where previous work [12] looks at the specific importance to precision machining control. To check the achieved rule set; tests are made against both seen and unseen test cases obtaining high confidence in classification accuracy.

3.3. Neural networks for precision control

A large number of researchers have reported the application of using NN models for the classification of phenomena of interest when applied to TCM [37,38]. The NN consists of complex interconnection of units which are otherwise known as nodes or neurons. The general layout for a NN consists of a set of neuron layers connected together through complex connections; such layout and features are known as the network architecture.

A multi-layer NN is required due to the more complex data presented by the summarised pre-processed signal data. This type of data is not only non-linear but also n-dimensional. The description, parameters and mechanics of the NN can be found in previous work [29] when back propagation learning rules were applied to a NN.

Warnecke and Kluge's research is of particular interest to the work presented in this paper as it uses NNs for the control of deviation errors when turning based on the AE measurements of tool flank wear [39]. This is where vibrations give a trace to deviations obtained from continuous machining with increasing wear states. These deviation errors are attributed to various parameters such as the change in temperature significant to increased flank tool wear and, the second attribution of backlash actuator errors. The research presented in this paper aims to give a capability and be able to do the same for micro-milling; controlling deviation errors.

4. AE technology used for precision machining

AE is finding more applications in industry, due to the possibility to measure a change in minute phenomena, however as calibration methods have not been accepted in terms of standardisation there needs to be more work in terms of its validation [40].

Hatano et al. [5] looked at pencil calibrations and various other calibration methods to investigate the AE elastic wave time/velocity and phase behaviour. Their investigation looked at both the transmitted and received signal. Hatano et al. [5] discusses spurious waves are not of huge significance compared to dominant waves (Raleigh and longitudinal: travel along the surface).

Using the raw extracted time and translated time frequency signal affords the user with a powerful control input for working in both real time and with good accuracy. With an extension of Fast Fourier Transforms (FFT) it is possible to get intensity and frequency band components for the analysed time interval. The FFT estimates the frequency components as well as their associated amplitudes based on the trigonometric family functions [41]. FFTs have been used for TCM in the past, however they do not define the time when the event occurred. This is fundamental to the nature of spontaneously-released transient elastic energy accompanying deformation or fracture of materials, or a combination of both [4], instead FFT has to be used alongside another technique that produces both the time and frequency band information.

Short Time Fourier Transforms (STFT) are a similar function to FFT, albeit the FFT is calculated for equally-spaced time slots designated across the raw extracted time signal. There is however a trade-off between frequency and time resolution. That said, and with the extra dimension of time, the STFT still offers a good solution when required to characterise an AE signal for precision control [12].

4.1. Acoustic emission statistical tests

For suitability and acceptance, statistical and regression analysis based on previous work where single grit scratch and pencil break tests were carried out to display the consistency of such technologies especially when confined to short distances [6].

Voltage amplitude instead of power decibel amplitude was considered more sensitive to change and therefore communicated here (where the measurement conversion was set to be 1 V per 1 μbar of pressure). The AE sensor used was a PAC wide band sensor and node acquisition system (70–1000 kHz).

5. Experimental setup of THz waveguide micro machining

5.1. Setup errors for THz micro machining

The achieved accuracy for the machine centre is currently 1 μm in the X and Y axis plane. As discussed previously, the Z axis accuracy is hovering around 4 μm. This is explained from the introduction of errors obtained from the zero setup condition (all CNC machines require initial setup). The error is introduced from the operator fixing the workpiece position for the first pass (Z=0). Current methods use a microscope with 40x magnification. To that end, possible problems of an incorrect level may exist as displayed by the setup in Fig. 1. The micro machine centre is driven by CNC code and over time other factors such as actuator backlash or wear of gears can occur, all contributing to the problems in achieving high precision. In the Z axis (direction of depth of cut) the machine centre is said to achieve an accuracy of 4 μm. However, the accuracy required for projects for higher frequencies should achieve 1 μm precision.

Using AE sensors, the signal energy levels increase with respect to more material removed (i.e. the tool takes an increasing cross-section of cut which is significant to an increasing change in removal rate experienced during the cut). Or, the opposite may be apparent if the setup error is made in the opposite direction. The critical factor here is the setup of the AE sensor and which axis is its orientation. Many publications discuss correlations with force sensors [33] however; the AE sensor is set up in the required machining cutting axis. When looking at such high precision levels it can be difficult to see such increasing or decreasing signal states, however previous work investigating micro, single grit material interaction displays such possibilities [6].

In short, the idea applied to this work seeks to achieve micron precision in the Z axis from information extracted via the AE measurements that could lead to the identification of the unlevelled point from its starting origin. Other irregularities such as defect anomalies or poor surface roughness can also be obtained from the same signals.

The signal error will facilitate the table setup and ensure the machined surface is level from one end to the other with no negative or positive gradients which is represented by decreasing or increasing AE signal intensities. With setup errors the micro tool dynamics become less predictable in terms of control, and lead to a diminishing surface quality and dimensional differences. In summary, this work ensures correct setup capabilities are possible where the tool could make a spring cut (0.1 mm) and the supplied signal would display if the machining/setup is level, or inclined either positively or negatively with respect to the Z axis. The monitoring of continuing DOC error from respective cuts allows the possibility for corrective spring cut(s) to ensure the final cut is

Table 1
Material characteristics duro-aluminium 6010.

Property	Duro-aluminium 6010
Composition (wt%)	Al: 97.3, Si: 1, Mg: 1=0.8, Mn: 0.5, Cu: 0.35
Hardness (HV)	88
Tensile strength (MPa)	290
Yield strength (Mpa=N/mm^2)	170
Elastic modulus (GPa)	69
Elongation (%)	24
Poisson's ratio	0.33

straight and level where the waveguide frequency characteristics are accurate and a high precision surface finish.

5.2. Setup for THz micro machining

Using a 5-axis Kern milling machine and an aluminium workpiece duro-aluminium alloy: Alumol 500 (Thyssen group: 6010, see Table 1 for more material characteristics). Four slots were cut in different configurations as shown in Fig. 3; a couplant gel was used between sensor and workpiece to promote superior Signal to Noise ratios.

The grooves were cut with a tungsten carbide micro-milling Dixi Polytool with 2 flutes and 0.5 mm diameter, where each pathway (see Figs. 2 and 8 for more information) consisted of an axial DOC of 0.3 mm for 6 passes and finally, 2 finishing cuts of 0.1 mm DOC. For each finishing cut with a DOC of 0.1 mm the surface of the groove walls consisted of two 0.1 mm DOC to produce the bottom surface, for the 0.3 DOC surface, two overlapping cuts were used to produce each 0.3 mm DOC surface (see Fig. 3). Fig. 3 displays the geometrical features and tolerances of the machined waveguide. The feedrate and spindle speeds for 0.3 mm DOC were 120 m/min and 15,000 RPM and for 0.1 mm DOC were 80 m/min and 20,000 RPM.

For verifying the machined surface quality, a Mitutoyo SJ-301 surface roughness tester and Carl Zeiss Stemi 2000 microscope were used to obtain measurements and images respectively.

6. Acoustic emission used to measure offset deviations and predict surface roughness

This section is split into two parts where the first looks at the AE signals and phenomena verification, the second part looks at geometrical deviation and surface roughness measurements for the fabrication of the THz waveguide.

6.1. AE analysis and phenomena verification

Firstly, the investigation of AE signal analysis is summarised in Fig. 4 which displays micro-milling test results (two performed with worn tools and two with new tools). It can be seen that the AE event towards the final cuts of the experiment (Tests 1 and 2) are experiencing large amplitudes compared to Tests 3 and 4 (using a new tool) which are significant to increasing tool wear tending towards catastrophic tool failure. This find is consistent with previous research investigating AE signals and tool wear of micro milling cutters [32]. From identifying these conditions, it was possible to use a threshold controller to state when the tool needed to be changed for a fresh tool. In addition, the same Tests suggest a capability in identifying setup errors where the Tests (3 and 4) display an increased error based on new tools confronted with a greater cross sectional area of material. As it is not standard practice to machine precision parts with a worn tool no CMM measurements were taken in these tests however this will be looked at in future work as it could become a significant factor if significant wear occurred during precision fabrication. If however wear limits exceed defined levels a command will be issued for tool swap out.

The next image, Fig. 5, displays the STFT of the machine passes reference to Test 4. Here a steady increase in AE can be seen which is indicative of the tool cutting on an inclined plane and therefore removing a proportionally increasing amount of material. The increase was not due to wear as Fig. 4 displays the differences between worn and non-worn tools (wear is based on obtaining higher amplitude amounts yet still varying in an increasing/decreasing uniform manner proportional to the cross sectional area of removed material however due to the higher amplitudes such signal ratios of level change maybe more difficult to identify).

The increasing axial depth of material being cut along the length of the slot is based on the tool moving in a level plane axis, albeit the workpiece was originally setup with a level error, hence the detected increasing AE amplitude. Fig. 5 shows an increasing error for the final Test and for the various machine passes. The penultimate pass (pass 7) of Fig. 5 displays less amplitude which is due to the smaller 0.1 mm spring cut (20 dB compared to 40 dB of the 0.3 mm DOC previous cuts). This spring cut is where the proposed error adjustments are applied to correct the geometrical deviation errors (during both final passes: 7 and 8).

Fig. 6 displays the maximum extracted amplitudes with respect to time for different machine passes relating to an increasing error significant to more energy released in terms of greater material removal rates based on the increasing error from the original setup conditions. It was noticed that when the tool was cutting in the groove wall, the waves were predominantly generated in the X

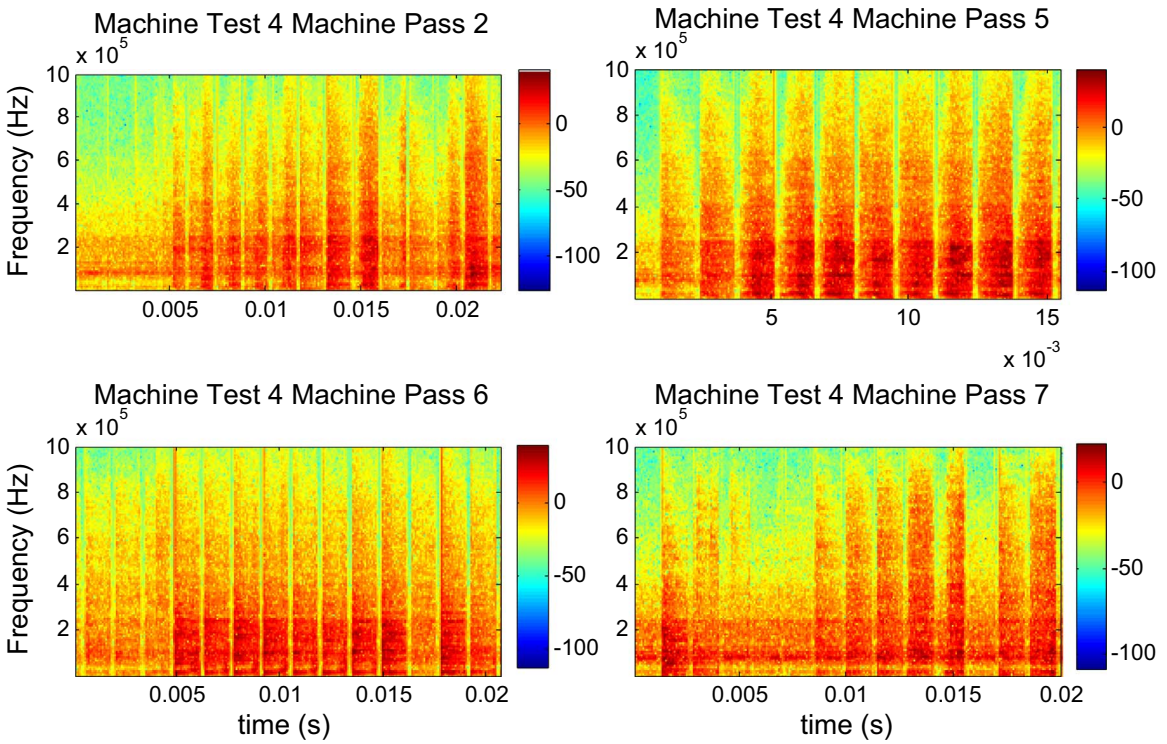

Fig. 5. STFT for Test 4 machine passes to produce the THz waveguide.

axis direction and the position of the sensor was more susceptible to AE stress-released waves, and as such these were noticed with greater intensity (these would be consistent at a specified interval along the tool path and diminish after passing that specific location). It was also noticed that as the tool distance from the sensor increased, greater signal intensities were recorded from various reflections and verberations. It was considered difficult if not impossible to correlate the signal with increased contact between the tool and material signifying an increasing error with respect to the initial workpiece set-up. Such mixed/ambiguous signals were ignored, and only the signals with the tool in approaching proximity to the sensor were considered.

6.2. *Deviation and surface roughness measurements of THz waveguide*

The following waveguide machining Tests relate to two different conditions, where the 1st and 2nd Tests relate to micro-milling

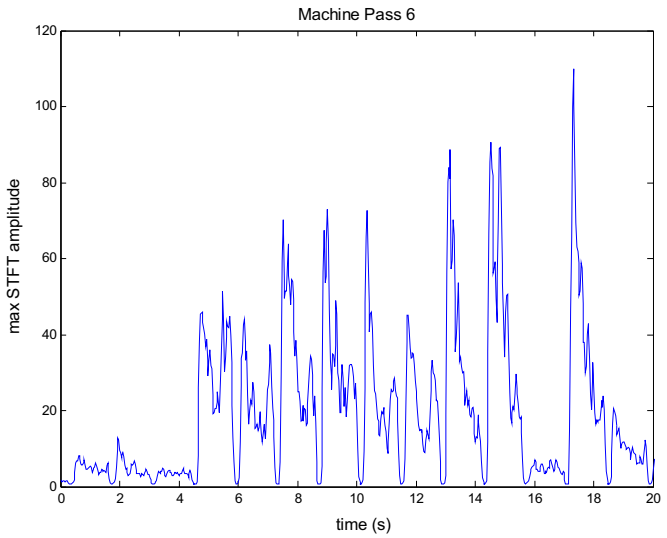

Fig. 6. Focused AE MAX amplitude of the STFT for Test 4 of selected pass (6).

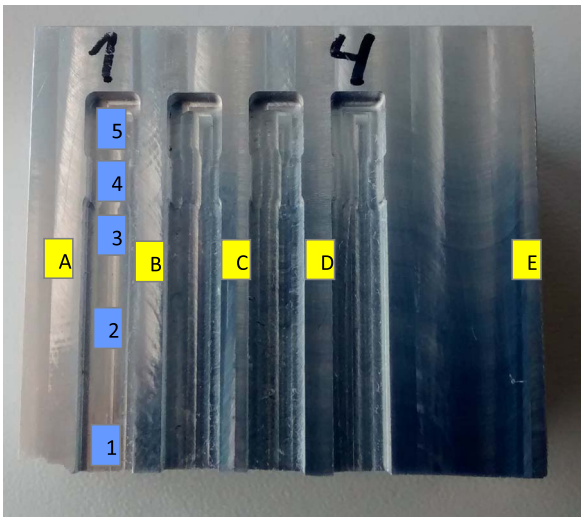

Fig. 7. Four waveguide manufacturing Tests, signifying measurement locations of surface roughness.

with a worn tool and the 3rd and 4th Tests are based on a new tool, to see the different effects obtained in respect of the cutting phenomena. Fig. 7 displays an image relating to the waveguide Tests carried out, where the top block numbers 1–4 relate to the individual groove tests and numbers inside the waveguide relate to individual roughness measurements (see Table 3 for corresponding results).

The micro CMM machine (Crysta Aplex C 122010) used for verifying the dimensions of the cut grooves (waveguides) is situated at the AMRC Sheffield University, Factory of the Future. The waveguides workpiece was datumed using a Plane-Line-Point alignment then the following were carried out:

- 4 points taken on top face to define the Z plane and origin.
- A line on left-hand side of part was inspected to create and artificial Y axis and set X origin.
- A point on the front face of the part was inspected to set the Y origin.
- The same features were inspected under CNC control for the final Datum/origin/co-ordinate system.
- The gauge points were 1, 10, 18, 21, 22, 22.5, 24.5, 26.25 and 27 mm respectively: both widths and depths of slots were made at the points.

Fig. 7 marking 'A' to 'E' are significant to 'Ra' measurement points for nominal horizontal material workpiece measurements. Table 2 displays the CMM for DOC and Width of Cut error measurements. Fig. 8 is a microscope image of the waveguide concentrator. It can be seen that the surface has consistent machining marks which again can contribute to the shortest path reference to signal following as opposed to direct path consistent with a high quality machined surface (typically in these trials the Ra was measured as 0.075 μm).

Looking at the values given by Table 3 the surface roughness measurements are consistent with milling and with a better finishing process as well as sensor-derived error mapping further improvements can be achieved.

Using a method of Wavelet Transforms (WT) via a secondary Simulink model (see Section 8) it was possible to use the AE extracted waveforms for the measure of average surface roughness (Ra). Where the following equation (Eq. (2)) was used to covert the high frequency AE vibrations to Ra measurements:

Table 2
Coordinate measurement machine (CMM) error values position in mm along waveguide.

	Slot 3			Slot4	
Ref markings (Fig. 7)	Position in mm	Depth of cut (DOC) error mm	Width of cut (WOC) error mm	DOC error mm	WOC error mm
	1 (start)	0.064	0.007	0.040	0.001
1	10	0.078	0.008	0.054	0.009
2	18	0.089	0.009	0.065	0.008
3	22	0.094	0.105	0.072	0.108
4	24.5	0.098	0.107	0.075	0.106
5	26.25	0.101	0.012	0.077	0.009
	27 (end)	0.102	0.010	0.078	0.006

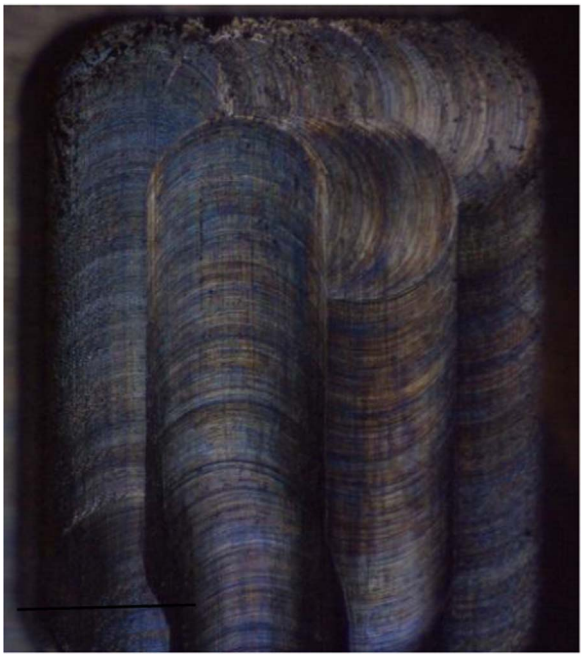

Fig. 8. Test 4, a focussed microscope image of the waveguide concentrator end part.

$$AE_{WT3} = \frac{1}{2n}\sum_{i=1}^{n}|y_i|^*\left|\frac{1}{AE_{Gain}}\right| \tag{2}$$

where the R_a is correlated with AE_{WT3} (AE wavelet transform (WT): level 3) which is transformed from its raw form and converted to the WT_{RMS} which becomes: y_i. This is then divided by two and multiplied by the inverse AE voltage gain to give the values as seen in Fig. 14 (using Kaiser window (see black dash-dot border on each given signal series) ensures no transients and ensures more accurate results). Fig. 14 displays two close up wavelet signatures for the final pass where correlations can be made back to the measured R_a values (see Table 3). This was based on previous works [42,43] Instead of using harmonics e^{-iwt}, as that seen in FFTs, the WT uses *wavelet basis* (Eq. (3)):

$$\psi_{ab}(t) = \frac{1}{\sqrt{a}}\psi\left(\frac{t-b}{a}\right) \tag{3}$$

where 'a' is scaling factor and 1/a represents the frequency (frequency bands decrease in bandwidth with respect to the different levels of WT: variable resolution when compared with static resolution; Short Time Fourier Transform). The *translation factor* 'b' is a time shift function and ψ(function) is known as the mother wavelet and is compactly supported. Eq. (4) displays an equation for the continuous wavelet function where a signal of interest x(t) is converted to the time-frequency domain with a scale 'a' and position 'b' [44].

Table 3
Ra measurements in μm, with reference to Fig. 7.

Wave guide 1 (Test 1)					
1	2	3	4	5	Average
0.14	0.15	0.17	0.16	0.19	0.16
Wave guide 2 (Test 2)					
1	2	3	4	5	Average
0.14	0.18	0.15	0.09	0.14	0.14
Wave guide 3 (Test 3)					
1	2	3	4	5	Average
0.13	0.12	0.08	0.12	0.15	0.12
Wave guide 4 (Test 4)					
1	2	3	4	5	Average
0.11	0.10	0.12	0.12	0.16	0.12

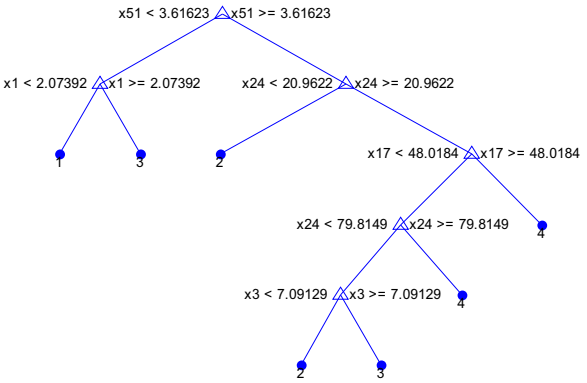

Fig. 9. CART classification tree for identifying the required control based on frequency band intensity.

$$w_f(a, b) = \frac{1}{\sqrt{a}} \int_{-\infty}^{\infty} x(t)\psi^*\left(\frac{t-b}{a}\right)dt \tag{4}$$

where * is the complex conjugation. The Simulink model (see Section 8) uses Eqs. (2) to (4) to represent the extracted AE signals into the time-frequency domain.

7. Classifications of deviation

Both classification systems can correlate the AE signals with the measured deviations of the micro-machined waveguides.

7.1. CART results

Fig. 9 relates to the normal CART rules (CART rules with added optimisation were also found). The CART rules are based on STFT AE signal for a given interval during a machine pass. The AE signals are based on a band of frequencies X1–X128 (70 kHz–1 MHz) and its specific power amplitude. The classification accuracy (test set) for the normal CART rules was 46/50 (92%), performing well as an accurate method for distinguishing different levels of AE relating to different levels of setup error. The training and test data are made up from the final pass data against the measured deviation (the training and test data is combined where the test cases have 66% unseen by the training data).

7.2. NN results (verifying control CART classifications)

Fig. 10 displays the same test data as used for the CART rules however this time applied to the NN model (verification test set). The result for the NN test set was 48/50 (96%) which again gives an encouraging set of results and suggests NN as a good verifier

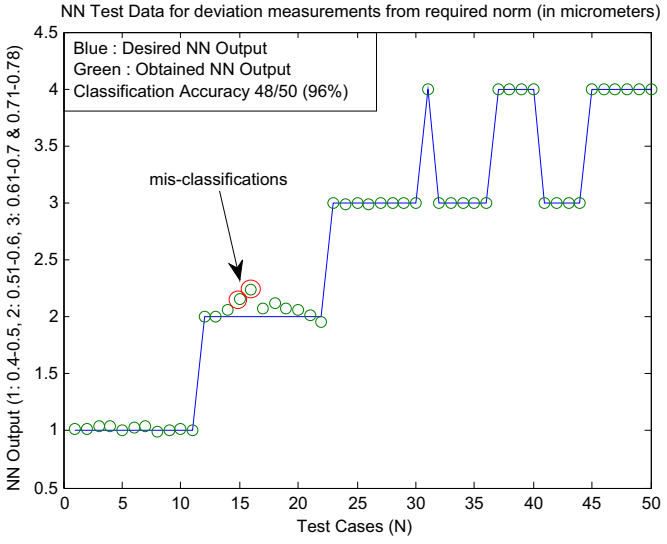

Fig. 10. NN classification test data for accurate deviation identification (all measurements *0.1 mm gain for correct measurement representation).

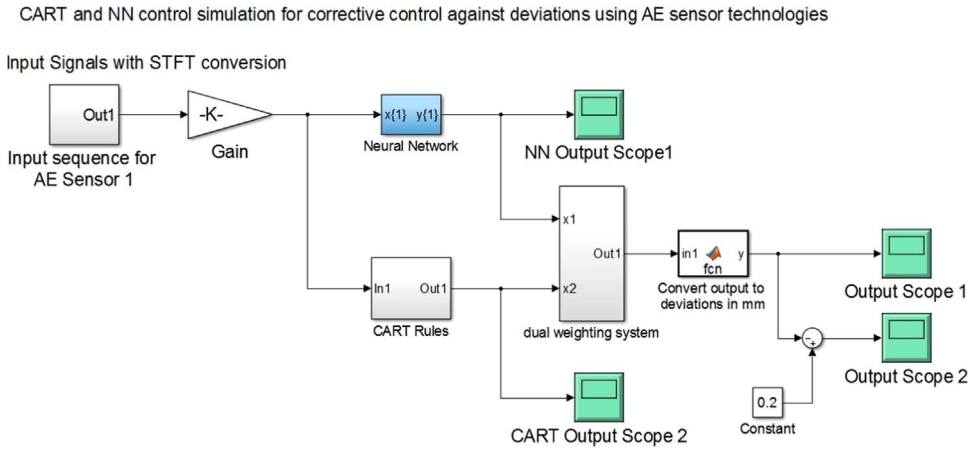

Fig. 11. Simulink simulation classification system for accurate deviation identification.

classifier technique for CART (not always the case [11]), albeit NN is more difficult to implement into embedded systems due to its computational complexity.

8. Real time controller for micro milling: deviations and surface roughness realised in a simulation

The simulation displayed in Fig. 11 displays a dual classifier system where the AE signal is transformed to the time-frequency domain using STFTs. After transformation, the signals pass a gain of intensity change, which is to simulate both increasing and decreasing error intensities. This enables the simulation to test for system robustness varying conditions to ensure generalised classification capabilities.

The simulation of Fig. 11 uses two classifiers for a more robust classification against possible sporadic outliers. It can be seen that the simulation is significant of an embedded electronic controller which would allow CNC code corrections for a deviation free surface with a near real-time response rate (note many measurements per time interval were made for the total duration of 20 s (see Fig. 12)). The type of internal architecture for the NN (simulation) can be found in previous work [27]. The last spring cuts apply the 0.1 mm DOC CNC correction, where the applied machining DOC would be 0.05 mm then 0.06 mm, followed by 0.07 mm to give the measured CNC taper correction based on the detected signal(s) (Fig. 12).

It was noticed that the AE signals obtained from the larger DOC were consistent with the small DOC displaying the same error albeit with less intensity significant of any emitted AE signal for a machining pass could be used as a reference for correction (see Fig. 5).

The following Figs. 13 and 14 display an extension to the Simulink deviation model where the same AE signals can be used to predict the surface roughness (Ra). The WT Simulink model is displayed in Fig. 13 . The reconstructed high frequency WT AE signals are displayed in Fig. 14 where signal (a) is significant to the AE signals at the beginning of extraction, (b) the middle and (c) the middle-end of extraction (all signals obtained during Test 4). Looking at Fig. 13 and applying Eqs. (2)–(4) and multiplying by an AE sensor gain it was possible to get within a small percentage of the measured surface roughness. This is very important considering the surface roughness is directly proportional to wave guide signal losses. The WT model uses a 3 level frequency analysis (more

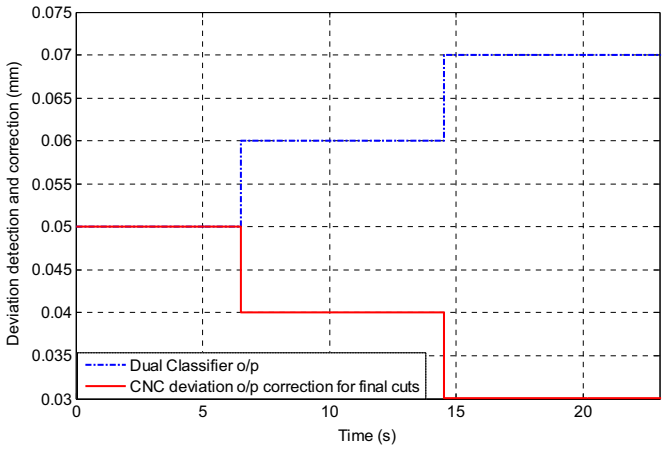

Fig. 12. Simulink simulation classification system output for accurate deviation identification.

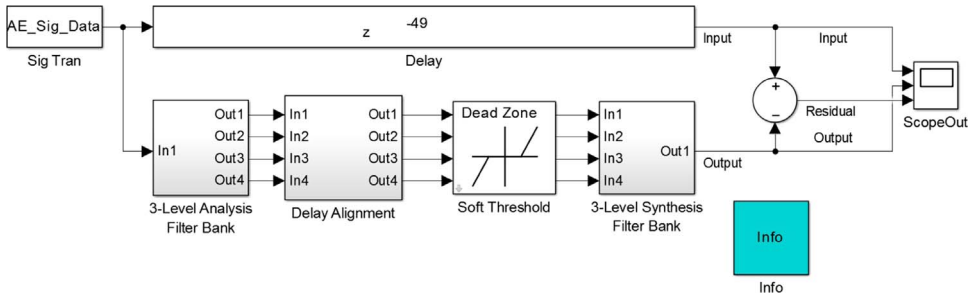

Fig. 13. Simulink wavelet transform model for NDE technique using AE to give surface roughness (Ra) measurements.

levels could be used however at a greater computational cost) to give the time-frequency information. The soft threshold acts as the wavelet function as seen in Eq. (4). The 3 level frequency analysis acts as a filter to allow specific frequencies which in this case are significant to machine tool interactions and enable surface roughness control.

9. Conclusions

The conclusions of this work are based on two major findings for micro-milling machine processes. The first finding is the increased amplitude of AE due to more energy identified when removing material with worn (blunt) tool. With greater wear levels the tool will remove less material which is significant to less energy being applied to the cutting process and therefore more energy is required to do the same effort of a sharp tool.

The other finding using maximum amplitudes of STFT energy mappings allow a mechanism to observe unlevel setup errors where an increasing energy is significant to positive level setup error and decreasing energy, significant to negative level setup error. The deviation mappings can be made to either change the setup error to the correct level (similar to a precision spirit level) or, produce corrective spring cuts to ensure level plane, deviation free surface are applied to the final spring cuts. The simulation provides a corrected level to the error deviation based on the extracted AE signal. In addition another simulation using the AE extracted signal information transforms to the time-frequency domain through WT and further transforms into the surface roughness (Ra) to give a measure of 'Ra' without the requirement of offline, difficult to make measurements. These results were consistent with sample measurements. The alignment of the AE sensors was found to be very important in terms of the cutting direction and should always be observed. For simulation of the deviation control both CART and NN gave good account as accurate robust controllers to work in conjunction with CNC machine controllers.

Future work will look deeper into the industrial issues as well as an actual physical implementation of reactive control based on embedded development. Some of the industrial issues could ensure more robustness and accuracy from mating with other technologies such a voltage probe as discussed [20]. The process of superior surface finish should look at a finishing process with a diamond abrasive tool as well as a more reactive heater control loop within the machining environment. A material thermocouple and AE sensor can be used to monitor the tool and workpiece condition in situ.

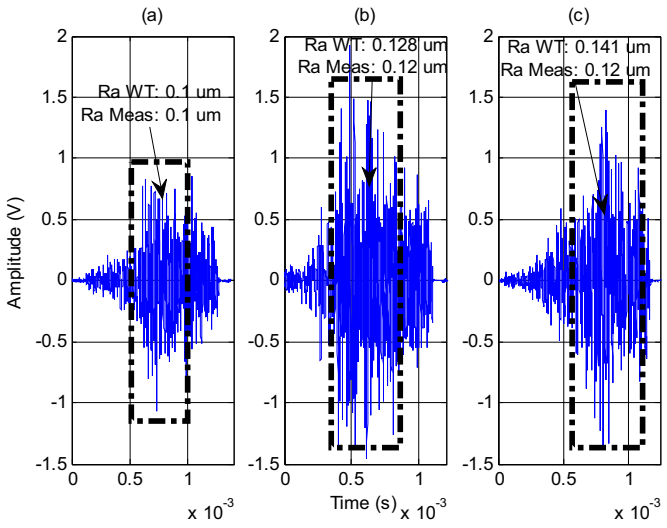

Fig. 14. Wavelet transform reconstruction: output from simulink model.

Acknowledgement

The authors are grateful to their colleagues in Cerro Calan, Chile José Santiago Pizarro Ormazábal. Please also note that the experimental work was carried out at Cerro Calán, University of Chile Astronomy Department, where FPM, EAM and LB acknowledge support through the Chilean Center for Excellence in Astrophysics and Associated Technologies (CONICYT Project CATA PFB-06). The authors are also grateful for the help and support (international placements and use of measuring equipment) given by the AMRC Sheffield University UK.

References

[1] K. Jemielniak, L. Kwiatkowski, P. Wrzosek, Diagnosis of tool wear based on cutting forces and acoustic emission measures as inputs to a neural network, J. Intell. Manuf. 9 (1998) 447–455.
[2] K. Popov, S. Dimov, A. Ivanov, D. Pham, E. Gandarias, New tool-workpiece setting up technology for micro-milling, Int. J. Adv. Manuf. Technol. 47 (2010) 21–27.
[3] M. Malekian, S.S. Park, M.B.G. Jun, Tool wear monitoring of micro-milling operations, J. Mater. Process. Technol. 209 (10) (2009) 4903–4914.
[4] L. Xiaoli, Tool wear monitoring with wavelet packet transform-fuzzy clustering method, Wear 219 (2) (1998) 145–154.
[5] H. Hatano, T. Chaya, S. Watanabe, K. Jinbo, Reciprocity calibration of impulse responses of acoustic emission transducers, IEEE Trans. Ultrason. Ferroelectron. Freq. Control 45 (5(12)) (1998) 1221–1228.
[6] J. Griffin, Traceability of acoustic emission measurements for a proposed calibration method – classification of characteristics and identification using signal analysis, Mech. Syst. Signal Process. 50–51 (2015) 757–783.
[7] L. Burke, S. Rangwala, Tool condition monitoring in metal cutting: a neural network approach, J. Intell. Manuf. 2 (1991) 269–280.
[8] L. Xiaoli, Y. Yingxue, Y. Zhejun, On-line tool condition monitoring system with wavelet fuzzy neural network, J. Intell. Manuf. 8 (1997) 271–276.
[9] K. Venkatesh, M. Zhou, R. Caudill, Design of neural networks for tool wear monitoring, J. Intell. Manuf. 8 (1997) 215–226.
[10] V. Sharma, S. Dhiman, R. Sehgal, S. Sharma, Estimation of cutting forces and surface roughness for hard turning using neural networks, J. Intell. Manuf. 8 (2008) 215–226.
[11] Q. Ren, L. Baron, M. Balazinski, K. Jemielniak, R. Botez, S. Achiche, Type-2 fuzzy tool condition monitoring system based on acoustic emission in micromilling, Inf. Sci. (2013).
[12] J. Griffin, F. Torres, Dynamic precision control in single-grit scratch tests using acoustic emission signals, Int. J. Adv. Manuf. Technol. (2015).
[13] R. Rodriguez, R. Finger, F.P. Mena, N. Reyes, E. Michael, L.A. Bronfman, Sideband-separating receiver with a calibrated digital IF-hybrid spectrometer for the millimeter band, Publ. Astron. Soc. Pac. 126 (938) (2014) 380–385.
[14] Khudchenko, A., Hesper, R., Baryshev, A., in: Proceedings of the 22nd International Symposium on Space Terahertz Technology, Tucson, 26–28, April (2011).
[15] M.G. Khan, A. Fartaj, A review on microchannel heat exchangers and potential applications, Int. J. Energy Res. 35 (2010) 553–582.
[16] P. Gunnasegaran, The effect of geometrical parameters on heat transfer characteristics of microchannels heat sink with different shapes, Int. Commun. Heat Mass Transf. 37 (2010) 1078–1086.
[17] M.H. Khadem, Numerical simulation of roughness effects on flow and heat transfer in microchannels at slip flow regime, Int. Commun. Heat Mass Transf. 36 (2009) 69–77.
[18] Narayanan G., Erickson N.R. and Gross R.M., Low cost direct machining of terahertz waveguide structures, in: Proceedings of the Tenth International Symposium on Space Terahertz Technology, Charlottesville, (2009), pp. 519–529.
[19] Narayanan G., Groppi C. and Chattopadhyay G., Waveguide Orthomode Transducer for 385–500 GHz, in: Proceedings of the 21st International Symposium on Space Terahertz Technology, Oxford, (2010), pp. 23–25
[20] Renishaw, Pocket guide to probing solutions for CNC machine tools, (2016), Available at ⟨www.renishaw.com⟩
[21] Mougo, A.L., Araujo, A.C. and Campos F.O., Effect of width of cut on micro milling aluminum alloy, in: Proceedings of the 22nd International Congress of Mechanical Engineering (COBEM 2013), Ribeirão Preto, SP, Brazil, (2013).
[22] A. Aramcharoen, P.T. Mativenga, Size effect and tool geometry in micro milling of tool, Precis. Eng. 33 (4) (2009) 402–407.
[23] W.Y. Bao, I.N. Tansel, Modeling micro end-milling operations. Part III: influence of tool wear, Int. J. Mach. Tools Manuf. (2000).
[24] F. Vollertsen, D. Biermann, H. Hansen, I. Jawahir, K. Kuzman, Size effects in manufacturing of metallic components, {CIRP} Ann. Manuf. Technol. 58 (2) (2009) 566–587.
[25] S.M. Afazov, D. Zdebski, S.M. Ratchev, J. Segal, S. Liu, Effects of micro milling conditions on the cutting forces and process stability, J. Mater. Process. Technol. 213 (2013) 671–684.
[26] M.P. Vogler, S.G. Kapoor, R.E. DeVor, On the modeling and analysis of machining performance in micro end milling, Part II: cutting force prediction, J. Manuf. Sci. Eng. 126 (2004) 695–705.
[27] A. Simoneau, E. Ng, M. Elbestawi, Grain size and orientation effects when microcutting {AISI} 1045 steel, {CIRP} Ann. Manuf. Technol. 56 (1) (2007) 57–60.
[28] Araujo, A.C., Mougo, A.L., Campos, F.O., Micro milling forces on machining aluminum alloy, in: Proceedings of the 8th International Conference on Micro Manufacturing – ICOMM2013, Victoria, Canada, (2013).
[29] Griffin J. and Chen X., Real-time simulation of neural network classifications from characteristics emitted by acoustic emission during horizontal single grit scratch tests, J. Intell. Manuf., Online ISSN1572-8145, (2014).
[30] D.A. Dornfeld, D.E. Lee, I. Hwang, C.M.O. Valente, J.F.G. Oliveira, Precision manufacturing process monitoring with acoustic emission, Int. J. Mach. Tools Manuf. 46 (2006) 176–18.
[31] Deshpande A. and Pieper R., Legacy machine monitoring using power signal analysis, in: Proceedings of the ASME 2011 International Manufacturing Science and Engineering Conference MSEC, Oregon, USA, (2011), pp. 1–8.
[32] K. Jemielniak, P.J. Arrazola, Application of AE and cutting force signals in tool condition monitoring in micro-milling, CIRP J. Manuf. Sci. Technol. 1 (2008) 97–102.
[33] I. Marinescu, D. Axinte, An automated monitoring solution for avoiding an increased number of surface anomalies during milling of aerospace alloys, Int. J. Mach. Tools Manuf. 51 (4) (2011) 349–357.
[34] L. Breiman, J. Friedman, R. Olshen, C. Stone. Classification and Regression Trees, Wadsworth, 1984.
[35] J. Hartigan, Statistical theory in clustering, J. Classif. 2 (1985) 63–76.
[36] D. Coppersmith, S.J. Hong, J.R.M. Hosking, Partitioning nominal attributes in decision trees, Data Min. Knowl. Discov. 3 (1999) 197–217.
[37] B. Sick, On-line and indirect tool wear monitoring in turning with artificial neural networks: a review of more than a decade of research, Mech. Syst. Signal Process. 16 (2002) 487–546.
[38] T. Ozel, Y. Karpat, Predictive modelling of surface roughness and tool wear in hard turning using regression and neural networks, Int. J. Mach. Tools Manuf. 45 (2005) 467–479.
[39] G. Warnecke, R. Kluge, Control of tolerances in turning by predictive control with neural networks, J. Intell. Manuf. 9 (1998) 281–287.
[40] M. Barbezat, A.J. Brunner, P. Flueler, C. Huber, X. Kornmann, Acoustic emission sensor properties of active fibre composite elements compared with commercial acoustic emission sensors, Sens. Actuators 114 (2004) 13–20.
[41] S.W. Smith, The Scientist and Engineer's Guide to Digital Signal Processing, California Technical Publishing, San Diego, 1997 ISBN 0-9660176-3-3.
[42] Beatriz de Agustina, Marta Marín, Roberto Teti, Eva Rubio, Surface roughness evaluation based on acoustic emission signals in robot assisted polishing, Sensors 14 (2014) 21514–21522.
[43] Dingtong Zhang and Ning Ding, Surface roughness intelligent prediction on grinding, in: Proceedings of the 3rd International Conference on Material, Mechanical and Manufacturing Engineering (IC3ME 2015), (2015).
[44] S.G. Mallat, A wavelet tour of signal processing, 2nd edition, Academic Press, San Diego, London, 1999.